HEAT TRANSFER EFFECTS IN A COUETTE FLOW THROUGH A COMPOSITE CHANNEL PARTLY FILLED BY A POROUS MEDIUM WITH A TRANSVERSE SINUSOIDAL INJECTION VELOCITY AND HEAT SOURCE

by

Dileep Singh CHAUHAN* and Vikas KUMAR

Department of Mathematics, University of Rajasthan, Jaipur-302004, India

*E-mail: dileepschauhan@gmail.com

This study theoretically analyzes the heat transfer effects in a three dimensional Couette flow through a composite parallel porous plate channel partly filled by a porous medium. The flow is three dimensional in the channel because of the application of a transverse sinusoidal injection velocity of a particular form at the lower stationary plate. The governing equations are solved using a perturbation series expansion method. The effects of various flow parameters such as, Prandtl number (Pr)*, suction/injection parameter* (λ)*, permeability of the porous medium* (K)*, heat source parameter* (S)*, and viscosity ratio parameter* (ϕ_1)*, are investigated on temperature distribution in the composite channel and rate of heat transfer at the upper moving plate and at the fluid-porous medium interface, and discussed graphically.*

Key words: *heat transfer, Couette flow, composite channel, porous medium, permeability.*

1. Introduction

The viscous fluid flow and heat transfer in porous medium is a topic of current research interest because of its numerous engineering, industrial and environmental applications. Such problems of flow and heat transfer through a wall-bounded porous medium in various types of ducts and channels, have been modeled using some variation of extended Darcy's equation, which describes a balance among pressure gradient, viscous transfer of momentum, linear or/and quadratic drag forces, by several researchers, e.g. Durlofsky and Brady [1], Kladias and Prasad [2], Vafai and Kim [3], Nakayama *et al.* [4], Nield *et al.* [5], Al-Hadhrami *et al.* [6], Kim and Russell [7], Nield *et al.* [8], Hooman *et al.* [9], Chauhan and Kumar [10].

The viscous fluid flow induced by a shearing motion of a wall in parallel-plate channel has been the subject of extensive research because of its numerous applications in many branches of science and technology. The velocity field for such flow usually serves a starting estimate for the velocity of more complex flows induced by convection and various boundary conditions. One of the fundamental fluid flow situations in porous medium and in channels partly filled with a porous substrate, is the Couette flow. Investigation of heat transfer in such flow in the presence of a porous medium has many important industrial applications, such as in chemical reactors, heat exchangers,

cooling and ceramic processing. Bhargava and Sacheti [11] examined heat transfer effects in Couette flow of two immiscible fluids through a porous channel using Darcy extended Brinkman equation to govern the flow. Daskalakis [12] studied Couette flow through a porous medium saturated by a high Prandtl number fluid and temperature dependent viscosity. Non-Darcy Couette flow is investigated by Nakayama [13] through a porous medium filled with an inelastic non-Newtonian fluid. Chauhan and Shekhawat [14], Chauhan and Vyas [15], investigated heat transfer effects in Couette flow of a compressible fluid in the presence of a naturally permeable boundary. Chauhan and Soni [16] examined parallel flow convection effects on Couette flow over a highly permeable bed. Kuznetsov [17] investigated analytically heat transfer effects in Couette flow in a porous medium using Darcy extended Brinkman-Forchheimer equation of momentum. Kuznetsov [18, 19] also analyzed fluid flow and heat transfer in Couette flow in a channel partly filled with a porous medium and partly with a clear fluid. Singh [20], Govindarajan *et al.* [21], Dass *et al.* [22] studied three-dimensional Couette flow and heat transfer in parallel-plate channel.

In this research, heat transfer effects are analyzed in three-dimensional Couette flow of a viscous fluid through a channel partly filled with a porous medium and partly with a clear fluid. In the composite channel lower part is occupied by a porous medium bounded by a porous plate where a transverse sinusoidal injection velocity is applied, and the upper part of the channel is occupied by a clear fluid. The upper porous plate of the channel moves with a constant velocity and a constant suction velocity is applied at it. The two boundary plates of the channel are kept at constant but different temperatures. The effects of the various parameters are examined on the temperature distribution and heat transfer rate.

2. Formulation of the problem

We consider viscous fluid Couette flow through a channel bounded by two infinite parallel porous plates, which are maintained at constant but different temperatures. The lower stationary porous plate is maintained at a temperature T_0', and a porous layer of thickness '*h*', is attached to it while the upper porous plate is maintained at a temperature T_1', and it moves at a constant distance '*d*' from the porous medium interface with constant velocity 'U_0'. It is also subjected to a constant suction velocity 'V_0'. The lower porous plate is subjected to a transverse sinusoidal injection velocity of the following form:

$$V = V_0\left(1+\varepsilon\cos\left(\pi z/d\right)\right), \tag{1}$$

where ε is a positive modulation parameter and $\varepsilon \ll 1$. The surface of the porous layer is taken horizontal in $x-z$ plane. The *x*-axis is taken in the flow direction and the y-axis is taken normal to the porous layer interface. Let (u,v,w,t) and (U,V,W,T) be the velocity and temperature components for the clear fluid region and porous medium region, respectively. All physical quantities are independent of *x*, since the channel is infinite in the *x*-direction.
We introduce the following non-dimensional quantities:

$$y^* = y/d\ ,\ z^* = z/d\ ,\ u^* = u/V_0\ ,\ v^* = v/V_0\ ,\ w^* = w/V_0\ ,\ U^* = U/V_0\ ,\ V^* = V/V_0\ ,W^* = W/V_0\ ,$$

$$t^* = \left(t - T_0'\right) \Big/ \left(T_1' - T_0'\right), T^* = \left(T - T_0'\right) \Big/ \left(T_1' - T_0'\right),\ p^* = p/\rho V_0^{\,2},\ P^* = P/\rho V_0^{\,2},\ K = K_0/d^2,\ a = h/d, \tag{2}$$

where, p, the pressure in clear-fluid region; P, the pressure in porous region; ρ, the density; and K_0 is the permeability of the porous medium.

Using above non-dimensional quantities, the governing dimensionless equations of the present problem, for flow and temperature distribution after dropping asterisks for convenience, are given by

$$\frac{\partial v}{\partial y} + \frac{\partial w}{\partial z} = 0, \tag{3}$$

$$v\frac{\partial u}{\partial y} + w\frac{\partial u}{\partial z} = \frac{1}{\lambda}\left(\frac{\partial^2 u}{\partial y^2} + \frac{\partial^2 u}{\partial z^2}\right), \tag{4}$$

$$v\frac{\partial v}{\partial y} + w\frac{\partial v}{\partial z} = -\frac{\partial p}{\partial y} + \frac{1}{\lambda}\left(\frac{\partial^2 v}{\partial y^2} + \frac{\partial^2 v}{\partial z^2}\right), \tag{5}$$

$$v\frac{\partial w}{\partial y} + w\frac{\partial w}{\partial z} = -\frac{\partial p}{\partial z} + \frac{1}{\lambda}\left(\frac{\partial^2 w}{\partial y^2} + \frac{\partial^2 w}{\partial z^2}\right), \tag{6}$$

$$v\frac{\partial t}{\partial y} + w\frac{\partial t}{\partial z} = \frac{1}{\lambda \,\mathrm{Pr}}\left(\frac{\partial^2 t}{\partial y^2} + \frac{\partial^2 t}{\partial z^2}\right) + St, \tag{7}$$

$$\frac{\partial V}{\partial y} + \frac{\partial W}{\partial z} = 0, \tag{8}$$

$$\phi_1\left(\frac{\partial^2 U}{\partial y^2} + \frac{\partial^2 U}{\partial z^2}\right) - \frac{U}{K} = 0, \tag{9}$$

$$\phi_1\left(\frac{\partial^2 V}{\partial y^2} + \frac{\partial^2 V}{\partial z^2}\right) - \frac{V}{K} = \lambda\frac{\partial P}{\partial y}, \tag{10}$$

$$\phi_1\left(\frac{\partial^2 W}{\partial y^2} + \frac{\partial^2 W}{\partial z^2}\right) - \frac{W}{K} = \lambda\frac{\partial P}{\partial z}, \tag{11}$$

$$V\frac{\partial T}{\partial y}+W\frac{\partial T}{\partial z}=\frac{\phi_2}{\lambda\,\mathrm{Pr}}\left(\frac{\partial^2 T}{\partial y^2}+\frac{\partial^2 T}{\partial z^2}\right)+ST\,. \tag{12}$$

The corresponding dimensionless boundary and matching conditions of the present problem are given by

$$y=1:\ \ u=A,\ \ v=1,\ \ w=0,\ \ t=1,$$

$$y=0:\ \ u=U,\ \ v=V,\ \ w=W,\ \ t=T,\ \ \ p=P,$$

$$\frac{\partial u}{\partial y}=\phi_1\frac{\partial U}{\partial y},\ \ \left(\frac{\partial v}{\partial z}+\frac{\partial w}{\partial y}\right)=\phi_1\left(\frac{\partial V}{\partial z}+\frac{\partial W}{\partial y}\right),\ \ \frac{\partial t}{\partial y}=\phi_2\frac{\partial T}{\partial y},$$

$$y=-a:\ \ U=0,\ \ V=\left(1+\varepsilon\cos\pi z\right),\ \ W=0\,,\ \ T=0, \tag{13}$$

where, $\phi_1=\bar{\mu}/\mu$; $\lambda=V_0 d/\nu$; $A=U_0/V_0$; $\mathrm{Pr}=\rho\nu C_p/k$; $\phi_2=\bar{k}/k$; $S=Qd/\rho C_p V_0$; $\nu=\mu/\rho$.

Here, μ, the viscosity; $\bar{\mu}$, the effective viscosity of the fluid in porous medium; ν, the kinematic viscosity; ϕ_1, the viscosity ratio; *k*, the thermal conductivity; $\bar{k}$, the effective thermal conductivity of the fluid in porous medium; ϕ_2, the thermal conductivity ratio; C_p, specific heat at constant pressure; *Q*, the heat source/sink; *S*, the source/sink parameter; *Pr*, the Prandtl number; and λ is the injection parameter.

3. Solutions

The flow problem can be solved by the perturbation series method, for very small values of the parameter $\varepsilon\left(\ll 1\right)$. We write

$$u(y,z)=u_0(y)+\varepsilon u_1(y,z)+\varepsilon^2 u_2(y,z)+.... \tag{14}$$

and similar expressions for *v, w, U, V, W, p* and *P*.

Here zeroth order solution $\left(\varepsilon=0\right)$ is simply the two dimensional coupled Couette flow in the channel with constant suction at the top and constant injection at the bottom. When $\varepsilon\neq 0$, we assume

$$u_1\left(y,z\right)=u_{11}\left(y\right)\cos\pi z\,,$$

$$v_1\left(y,z\right)=v_{11}\left(y\right)\cos\pi z\,,$$

$$w_1\left(y,z\right)=-\frac{1}{\pi}v_{11}'\left(y\right)\sin\pi z\,,$$

$$p_1(y,z) = p_{11}(y)\cos\pi z\,,$$

$$U_1(y,z) = U_{11}(y)\cos\pi z\,,$$

$$V_1(y,z) = V_{11}(y)\cos\pi z\,,$$

$$W_1(y,z) = -\frac{1}{\pi}V_{11}'(y)\sin\pi z\,,$$

$$P_1(y,z) = P_{11}(y)\cos\pi z\,.$$

Velocity and pressure distributions are obtained under the corresponding boundary conditions, (Chauhan and Kumar [23]).

3.1 *Heat Transfer Analysis*

For solving the energy equations (7) and (12), we write

$$t(y,z) = t_0(y) + \varepsilon t_{11}(y)\cos\pi z\,, \tag{15}$$

$$T(y,z) = T_0(y) + \varepsilon T_{11}(y)\cos\pi z\,. \tag{16}$$

Substituting (15) and (16) into equations (7), (12) and the corresponding boundary conditions (13), comparing the coefficients of equal powers of ε on both sides, and then solving the resulting set of ordinary equations under the corresponding boundary conditions, we obtain

$$\begin{aligned} t(y,z) &= a_1\exp(\alpha_1 y) + a_2\exp(\alpha_2 y) + \varepsilon\left(a_5\exp(\alpha_5 y) + a_6\exp(\alpha_6 y)\right)\cos\pi z \\ &+\varepsilon\lambda Pr\left[a_1\alpha_1\left(\frac{A_1\exp\left((\pi+\alpha_1)y\right)}{l_1} + \frac{A_2\exp\left((-\pi+\alpha_1)y\right)}{l_2} + \frac{A_3\exp\left((r_1+\alpha_1)y\right)}{l_3} + \frac{A_4\exp\left((r_2+\alpha_1)y\right)}{l_4}\right)\right. \\ &\left.+a_2\alpha_2\left(\frac{A_1\exp\left((\pi+\alpha_2)y\right)}{l_5} + \frac{A_2\exp\left((-\pi+\alpha_2)y\right)}{l_6} + \frac{A_3\exp\left((r_1+\alpha_2)y\right)}{l_7} + \frac{A_4\exp\left((r_2+\alpha_2)y\right)}{l_8}\right)\right]\cos\pi z, \end{aligned} \tag{17}$$

and

$$T(y,z)=a_3\exp(\alpha_3 y)+a_4\exp(\alpha_4 y)+\varepsilon\left(a_7\exp(\alpha_7 y)+a_8\exp(\alpha_8 y)\right)\cos\pi z$$

$$+\varepsilon\lambda\,\mathrm{Pr}\left[a_3\alpha_3\left(\begin{array}{l}\dfrac{B_1\exp\left((\pi+\alpha_3)y\right)}{l_9}+\dfrac{B_2\exp\left((-\pi+\alpha_3)y\right)}{l_{10}}\\+\dfrac{B_3\exp\left((s+\alpha_3)y\right)}{l_{11}}+\dfrac{B_4\exp\left((-s+\alpha_3)y\right)}{l_{12}}\end{array}\right)\right.$$

$$\left.+a_4\alpha_4\left(\begin{array}{l}\dfrac{B_1\exp\left((\pi+\alpha_4)y\right)}{l_{13}}+\dfrac{B_2\exp\left((-\pi+\alpha_4)y\right)}{l_{14}}\\+\dfrac{B_3\exp\left((s+\alpha_4)y\right)}{l_{15}}+\dfrac{B_4\exp\left((-s+\alpha_4)y\right)}{l_{16}}\end{array}\right)\right]\cos\pi z. \qquad (18)$$

Where,

$$\alpha_1=\frac{\lambda Pr+\sqrt{\lambda^2Pr^2-4S\lambda Pr}}{2},\quad \alpha_2=\frac{\lambda Pr-\sqrt{\lambda^2Pr^2-4S\lambda Pr}}{2},$$

$$\alpha_3=\frac{\lambda Pr+\sqrt{\lambda^2Pr^2-4S\phi_2\lambda Pr}}{2\phi_2},\quad \alpha_4=\frac{\lambda Pr-\sqrt{\lambda^2Pr^2-4S\phi_2\lambda Pr}}{2\phi_2},$$

$$\alpha_5=\frac{\lambda Pr+\sqrt{\lambda^2Pr^2-4\left(S\lambda Pr-\pi^2\right)}}{2},\quad \alpha_6=\frac{\lambda Pr-\sqrt{\lambda^2Pr^2-4\left(S\lambda Pr-\pi^2\right)}}{2},$$

$$\alpha_7=\frac{\lambda Pr+\sqrt{\lambda^2Pr^2-4\phi_2\left(S\lambda Pr-\phi_2\pi^2\right)}}{2\phi_2},\quad \alpha_8=\frac{\lambda Pr-\sqrt{\lambda^2Pr^2-4\phi_2\left(S\lambda Pr-\phi_2\pi^2\right)}}{2\phi_2},$$

and $a_1, a_2, a_3, a_4, a_5, a_6, a_7, a_8$ are constants of integrations. These constants have been obtained by the boundary and matching conditions and are reported in the Appendix.

The dimensionless rate of heat transfer at the moving plate and at the fluid-porous medium interface, are given by

$$\left(\frac{\partial t}{\partial y}\right)_{y=1}=t'(1)=a_1\alpha_1\exp(\alpha_1)+a_2\alpha_2\exp(\alpha_2)+\varepsilon\left(a_5\alpha_5\exp(\alpha_5)+a_6\alpha_6\exp(\alpha_6)\right)\cos\pi z$$

$$+\varepsilon\lambda Pr\left[a_1\alpha_1\left(\begin{array}{l}\dfrac{A_1(\pi+\alpha_1)\exp(\pi+\alpha_1)}{l_1}+\dfrac{A_2(-\pi+\alpha_1)\exp(-\pi+\alpha_1)}{l_2}\\+\dfrac{A_3(r_1+\alpha_1)\exp(r_1+\alpha_1)}{l_3}+\dfrac{A_4(r_2+\alpha_1)\exp(r_2+\alpha_1)}{l_4}\end{array}\right)\right.$$

$$+a_2\alpha_2\left[\begin{array}{l}\dfrac{A_1(\pi+\alpha_2)\exp(\pi+\alpha_2)}{l_5}+\dfrac{A_2(-\pi+\alpha_2)\exp(-\pi+\alpha_2)}{l_6}\\ +\dfrac{A_3(r_1+\alpha_2)\exp(r_1+\alpha_2)}{l_7}+\dfrac{A_4(r_2+\alpha_2)\exp(r_2+\alpha_2)}{l_8}\end{array}\right]\cos\pi z, \tag{19}$$

and

$$\left(\frac{\partial t}{\partial y}\right)_{y=0}=t'(0)=a_1\alpha_1+a_2\alpha_2+\varepsilon\left(a_5\alpha_5+a_6\alpha_6+m_5\right)\cos\pi z\,. \tag{20}$$

4. Discussion

Figure 1 depicts the temperature distribution in the channel for different values of the Prandtl number *Pr*. On comparing the various curves in the fig., it is observed that the effect of Prandtl number is to decrease the temperature at all points in the flow field of the composite channel. In fact, the thermal conduction, in flow field of both the regions, is lowered as we increase the value of the Prandtl number, and there is a decrease in the molecular motion of the fluid elements, consequently the temperature falls in the channel. Figure 2 shows the effect of suction/injection parameter λ on the temperature distribution in the channel. When λ is very small, the temperature profile is nearly linear. As the value of λ increases, more amount of fluid is pushed into the channel through the lower plate, causing a decrease in temperature at all points in the channel. Figure 3, however, shows that the source parameter *S* increases the temperature in the channel at all points.

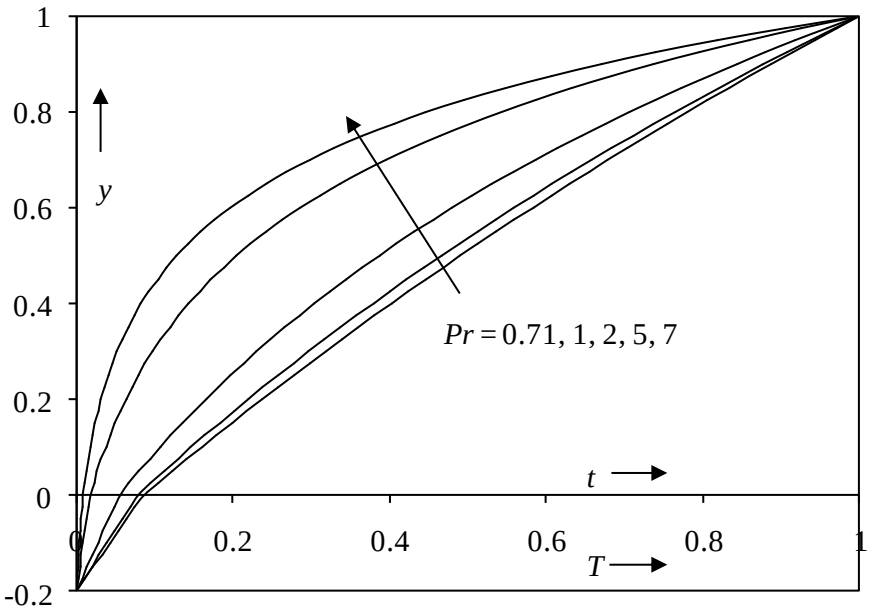

Fig. 1. Temperature profile against *y* for $\lambda=0.5,\ S=-0.5,\ a=0.2,\ \phi_2=1.666,\ K=0.1, \phi_1=1.25$ $\varepsilon=0.1,\ z=0$.

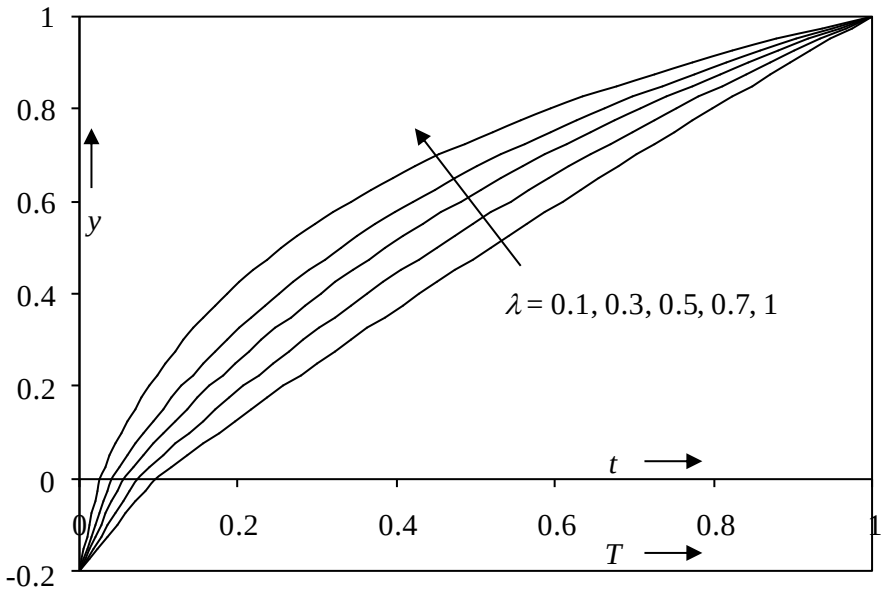

Fig. 2. Temperature profile against *y* for $Pr = 2,\ S = -0.5,\ a = 0.2,\ \phi_2 = 1.666,\ K = 0.1, \phi_1 = 1.25$ $\varepsilon = 0.1,\ z = 0$.

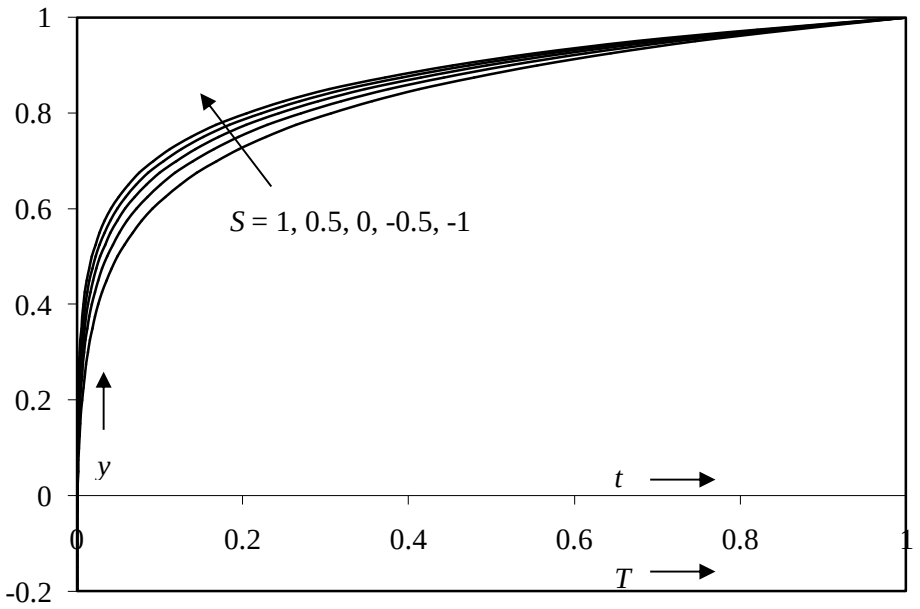

Fig. 3. Temperature profile against *y* for $\lambda = 1,\ Pr = 7,\ a = 0.2,\ \phi_2 = 1.666,\ K = 0.1, \phi_1 = 1.25$ $\varepsilon = 0.1,\ z = 0$.

The variations in temperature profiles in the composite channel for different values of the permeability K and viscosity ratio ϕ_1 are depicted in tab. 1 and 2 respectively. It is found that temperature increases in the composite channel at each y as the permeability K increases. Since the

porous layer is highly permeable, increase in the value of K causes increase in the flow velocity and so due to friction temperature in the channel also rises. Similarly increase in the viscosity ratio parameter ϕ_1 causes rise in the temperature in the channel.

Table 1. Temperature distribution for $Pr = 2, S = -0.5, a = 0.2, \phi_2 = 1.666, \lambda = 0.5, \phi_1 = 1.25, \varepsilon = 0.1, z = 0$.

Y	$K = 0.0001$	$K = 0.001$	$K = 0.01$	$K = 0.1$	$K = 1$
-0.2	0	0	0	0	0
-0.1	0.026363	0.026372	0.026393	0.026401	0.026403
0	0.054523	0.054548	0.054598	0.054618	0.05462
0.1	0.106309	0.106357	0.106445	0.106477	0.106481
0.2	0.16437	0.164442	0.164567	0.16461	0.164616
0.3	0.229633	0.229725	0.229876	0.229928	0.229935
0.4	0.303158	0.303261	0.303427	0.303482	0.303489
0.5	0.38616	0.386265	0.386431	0.386486	0.386493
0.6	0.480036	0.480133	0.480284	0.480334	0.48034
0.7	0.586383	0.586464	0.586588	0.586629	0.586634
0.8	0.707035	0.707093	0.707181	0.70721	0.707214
0.9	0.844098	0.844128	0.844174	0.844189	0.844191
1	1	1	1	1	1

Table 2. Temperature distribution for $Pr = 2, S = -0.5, a = 0.2, \phi_2 = 1.666, \lambda = 0.5, K = 0.1, \varepsilon = 0.1, z = 0$.

y	$\phi_1 = 1$	$\phi_1 = 1.25$	$\phi_1 = 2$	$\phi_1 = 4$	$\phi_1 = 6$
-0.2	0	0	0	0	0
-0.1	0.026399	0.026402	0.026412	0.026428	0.026436
0	0.054611	0.054619	0.054641	0.054674	0.054691
0.1	0.106466	0.106479	0.106513	0.106566	0.106593
0.2	0.164595	0.164613	0.164659	0.164728	0.164762
0.3	0.229911	0.229932	0.229985	0.230065	0.230104
0.4	0.303463	0.303487	0.303543	0.303627	0.303668
0.5	0.386467	0.38649	0.386545	0.386627	0.386667
0.6	0.480317	0.480338	0.480388	0.480461	0.480497
0.7	0.586615	0.586632	0.586673	0.586733	0.586762
0.8	0.7072	0.707212	0.707241	0.707283	0.707304
0.9	0.844184	0.84419	0.844205	0.844227	0.844238
1	1	1	1	1	1

Figure 4 and 5 shows the variation of the rate of heat transfer at the upper moving plate and at the porous interface. We see that the Prandtl number (*Pr*) is found to enhance the rate of heat transfer at the upper moving plate of the channel. So is the case with the suction/injection parameter λ, where as *Pr* or λ decreases the rate of heat transfer at the fluid-porous medium interface. Further it is noticed that heat source parameter causes decrease in the rate of heat transfer at the upper plate, while reverse effects observed at the fluid-porous medium interface.

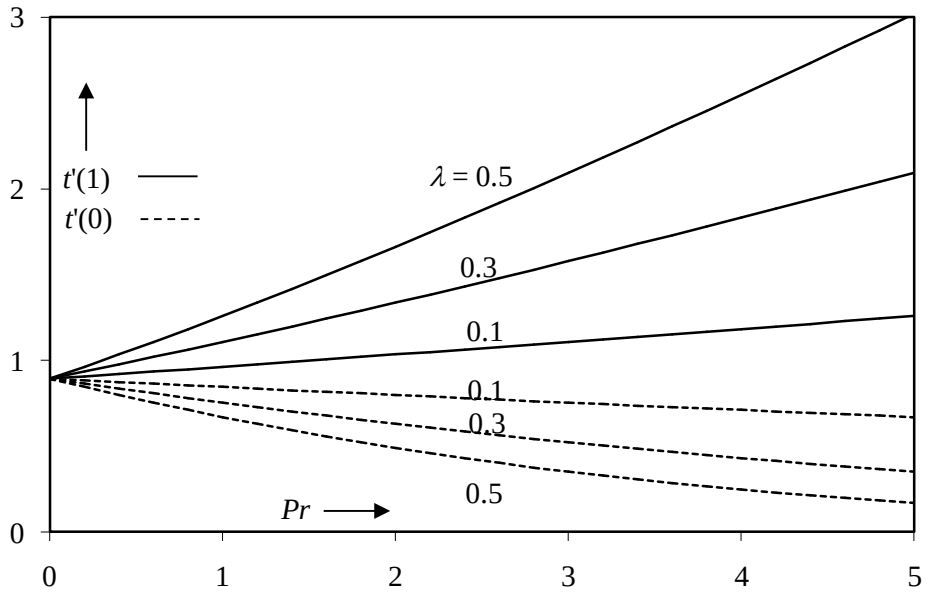

Fig. 4. Rate of heat transfer against *Pr* for $K = 0.1,\ \varepsilon = 0.1,\ \phi_1 = 1.25,\ a = 0.2,\ S = -0.5,\ z = 0$.

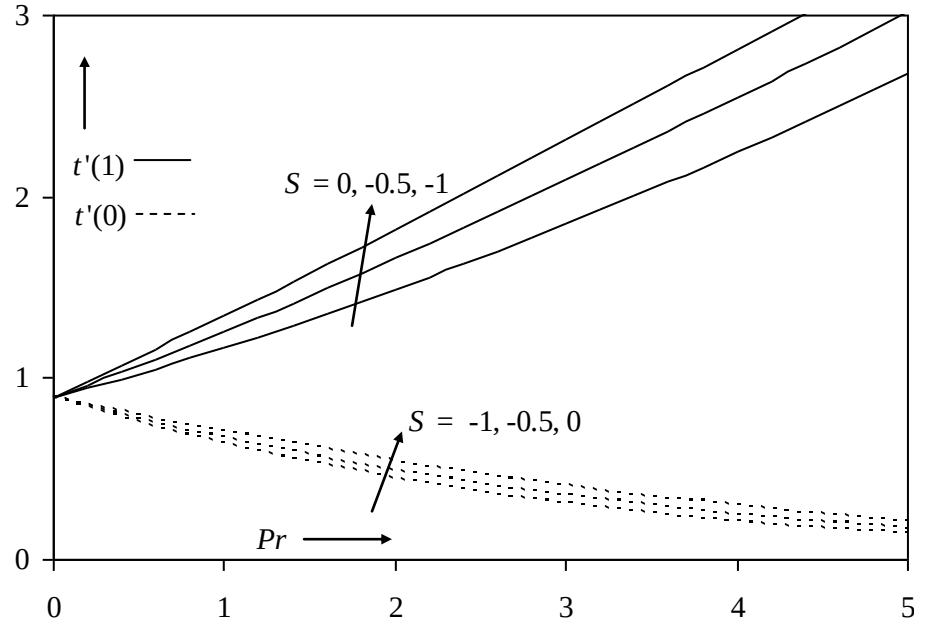

Fig. 5. Rate of heat transfer against *Pr* for $K = 0.1,\ \varepsilon = 0.1,\ \phi_1 = 1.25,\ a = 0.2,\ \lambda = 0.5,\ z = 0$.

Table 3(a-b) and 4(a-b) depict the effects of the permeability K and the viscosity ratio parameter ϕ_1 as the rate of heat transfer at the upper moving plate and at the porous interface. It is found that the rate of heat transfer increases with the increase in the value of K or ϕ_1 at the fluid-porous interface, whereas opposite results are observed at the upper moving plate.

Table 3(a) Rate of heat transfer at the upper plate, $t'(1)$ for $\lambda = 0.5, \varepsilon = 0.1, \phi_1 = 1.25, a = 0.2,$ $S = -0.5$.

Pr	$K = 1$	$K = 0.1$	$K = 0.01$	$K = 0.001$
0.71	1.148549	1.148555	1.148604	1.148755
1	1.258733	1.258743	1.258813	1.259033
2	1.661271	1.661291	1.661447	1.66193
5	3.018797	3.018853	3.019283	3.020632
7	3.991178	3.991254	3.99184	3.993687

Table 3(b) Rate of heat transfer at the upper plate, $t'(1)$ for $\lambda = 0.5, \varepsilon = 0.1, K = 0.1, a = 0.2,$ $S = -0.5$.

Pr	$\phi_1 = 1.25$	$\phi_1 = 2$	$\phi_1 = 4$	$\phi_1 = 6$
0.71	1.148555	1.148506	1.148434	1.148399
1	1.258743	1.258671	1.258567	1.258516
2	1.661291	1.661136	1.660908	1.660797
5	3.018853	3.018426	3.017802	3.017498
7	3.991254	3.990673	3.989829	3.989418

Table 4(a) Rate of heat transfer at the upper plate, $t'(0)$ for $\lambda = 0.5, \varepsilon = 0.1, \phi_1 = 1.25, a = 0.2,$ $S = -0.5$.

Pr	$K = 1$	$K = 0.1$	$K = 0.01$	$K = 0.001$
0.71	0.729661	0.729653	0.729596	0.729437
1	0.669473	0.669463	0.669388	0.669175
2	0.489955	0.489938	0.489817	0.489473
5	0.169944	0.169926	0.169789	0.169401
7	0.077553	0.077539	0.077439	0.077151

Table 4(b) Rate of heat transfer at the upper plate, $t'(0)$ for $\lambda = 0.5$, $\varepsilon = 0.1$, $K = 0.1$, $a = 0.2$, $S = -0.5$.

Pr	$\phi_1 = 1.25$	$\phi_1 = 2$	$\phi_1 = 4$	$\phi_1 = 6$
0.71	0.729653	0.729712	0.729803	0.729848
1	0.669463	0.669542	0.669662	0.669723
2	0.489938	0.490065	0.49026	0.490357
5	0.169926	0.170068	0.170286	0.170395
7	0.07754	0.077644	0.077805	0.077885

Acknowledgement

The authors are thankful to the referee for his valuable comments and suggestions. The support provided by Council of Scientific and Industrial Research through Senior Research Fellowship to one of the authors Vikas Kumar is gratefully acknowledged.

References

[1] Durlofsky, L., Brady, J. F., Analysis of the Brinkman equation as a model for flow in porous media, *Phys. Fluids, 30* (1987), pp. 3329-3341.

[2] Kladias, N., Prasad, V., Experimental verification of DBF flow model for natural convection in porous media: A case study for horizontal layers, *AIAA Journal of Thermophysics and Heat Transfer, 5* (1991), pp. 560-576.

[3] Vafai, K., Kim, S. J., Forced convection in a channel filled with a porous medium: an exact-solution, *ASME J. Heat Transfer, 111* (1989), pp. 1103-1106.

[4] Nakayama, A., Koyama, H., Kuwahara, F., An analysis on forced convection in a channel filled with a Brinkman-Darcy porous medium: Exact and approximate solutions, *Wärme-und Stoffübertragung, 23* (1988), pp. 291-295.

[5] Nield, D. A., Junqueira, S. L. M., Lage, J. L., Forced convection in a fluid saturated porous medium channel with isothermal or isoflux boundaries, *J. Fluid Mech., 322* (1996), pp. 201-214.

[6] Al-Hadhrami, A. K., Elliott, L., Ingham, D. B., Combined free and forced convection in vertical channels of porous media, *Transport in Porous Media, 49* (2002), pp. 265-289.

[7] Kim, S., Russell, W. B., Modeling of porous media by renormalization of the Stokes equation, *J. Fluid Mech., 154* (1985), 269-286.

[8] Nield, D. A., Kuznetsov, A. V., Xiong, M., Effects of viscous dissipation and flow work on forced convection in a channel filled by a saturated porous medium, *Transport in Porous Media, 56* (2004), pp. 351-367.

[9] Hooman, K., Gurgenci, H., Merrikh, A. A., Heat transfer and entropy generation optimization of forced convection in a porous-saturated duct of rectangular cross-section, *Int. J. Heat and Mass Transfer, 50* (2007), pp. 2051-2059.

[10] Chauhan, D. S., Kumar, V., Effects of slip condition on forced convection and entropy generation in a circular channel occupied by a highly porous medium: Darcy extended Brinkman-Forchheimer model, *Turkish J. Eng. Env. Sci., 33* (2009), pp. 91-104.
[11] Bhargava, S. K., Sacheti, N. C., Heat transfer in generalized Couette flow of two immiscible Newtonian fluids through a porous channel: use of Brinkman model, *Indian J. Tech., 27* (1989), pp. 211-214.
[12] Daskalakis, J., Couette flow through a porous medium of a high Prandtl number fluid with temperature dependent viscosity, *Int. J. of Energy Research, 14* (1990), pp. 21-26.
[13] Nakayama, A., Non-Darcy Couette flow in a porous medium filled with an inelastic non-Newtonian fluid, *ASME Journal of Fluids Engineering, 114* (1992), pp. 642-647.
[14] Chauhan, D. S., Shekhawat, K. S., Heat transfer in Couette flow of a compressible Newtonian fluid in the presence of a naturally permeable boundary, *J. Phys. D: Appl. Phys., 26* (1993), pp. 933-936.
[15] Chauhan, D. S., Vyas, P., Heat transfer in hydromagnetic Couette flow of compressible Newtonian fluid, *ASCE Journal of Engineering Mechanics, 121* (1995), 1, pp. 57-61.
[16] Chauhan, D. S., Soni, V., Parallel flow convection effects on Couette flow past a highly porous bed, *Modeling, Measurement & Control, B, AMSE Press, 56* (1994), 1, pp. 7-21.
[17] Kuznetsov, A. V., Analytical investigation of Couette flow in a composite channel partially filled with a porous medium and partially with a clear fluid, *Int. J. Heat Mass Transfer, 41* (1998), 16, pp. 2556-2560.
[18] Kuznetsov, A. V., Analytical investigation of heat transfer in Couette flow through a porous medium utilizing the Brinkman-Forchheimer-extended Darcy model, *Acta Mechanica, 129* (1998), pp. 13-24.
[19] Kuznetsov, A. V., Fluid flow and heat transfer analysis of Couette flow in a composite duct, *Acta Mech., 140* (2000), pp. 163–170.
[20] Singh, K. D., Three dimensional Couette flow with transpiration cooling, *ZAMP, 50* (1999), pp. 661-668.
[21] Govindarajan, A., Ramamurthy, V., Sundarammal, K., 3D Couette flow of dusty fluid with transpiration cooling, *Journal of Zhejiang University SCIENCE A, 8* (2007), 2, pp. 313-322.
[22] Das, S. S., Mohanty, M., Panda, J. P., Sahoo, S. K., Hydromagnetic three dimensional Couette flow and heat transfer, *J. of Naval Architecture and Marine Engng., 5* (2008), pp. 1-10.
[23] Chauhan, D. S., Kumar, V., Three-dimensional Couette flow in a composite channel partially filled with a porous medium, *Appl. Math. Sci., 4* (2010), 54, pp. 2683-2695.

Appendix

$$\alpha = \left(\alpha_1 \mathrm{e}^{\alpha_2} - \alpha_2 \mathrm{e}^{\alpha_1}\right)\left(\mathrm{e}^{\mathrm{a}\alpha_3} - \mathrm{e}^{\mathrm{a}\alpha_4}\right) - \phi_2\left(\mathrm{e}^{\alpha_2} - \mathrm{e}^{\alpha_1}\right)\left(\alpha_3 \mathrm{e}^{\mathrm{a}\alpha_3} - \alpha_4 \mathrm{e}^{\mathrm{a}\alpha_4}\right),$$

$$\mathrm{a}_1 = \frac{\phi_2\left(\alpha_3 \mathrm{e}^{\mathrm{a}\alpha_3} - \alpha_4 \mathrm{e}^{\mathrm{a}\alpha_4}\right) - \alpha_2\left(\mathrm{e}^{\mathrm{a}\alpha_3} - \mathrm{e}^{\mathrm{a}\alpha_4}\right)}{\alpha},\ \mathrm{a}_2 = \mathrm{e}^{-\alpha_2}\left(1 - \mathrm{a}_1 \mathrm{e}^{\alpha_1}\right),$$

$$\mathrm{a}_3 = \frac{\mathrm{e}^{\mathrm{a}\alpha_3 - \alpha_2}}{\left(\mathrm{e}^{\mathrm{a}\alpha_3} - \mathrm{e}^{\mathrm{a}\alpha_4}\right)}\left(1 + \mathrm{a}_1\left(\mathrm{e}^{\alpha_2} - \mathrm{e}^{\alpha_1}\right)\right),\ \mathrm{a}_4 = -\mathrm{a}_3 \mathrm{e}^{-\mathrm{a}(\alpha_3 - \alpha_4)},$$

$$l_1=(\pi+\alpha_1)^2-\lambda\,\mathrm{Pr}(\pi+\alpha_1)+S\lambda\,\mathrm{Pr}-\pi^2,\ l_2=(-\pi+\alpha_1)^2-\lambda\,\mathrm{Pr}(-\pi+\alpha_1)+S\lambda\,\mathrm{Pr}-\pi^2,$$

$$l_3=(r_1+\alpha_1)^2-\lambda\,\mathrm{Pr}(r_1+\alpha_1)+S\lambda\,\mathrm{Pr}-\pi^2,\ l_4=(r_2+\alpha_1)^2-\lambda\,\mathrm{Pr}(r_2+\alpha_1)+S\lambda\,\mathrm{Pr}-\pi^2,$$

$$l_5=(\pi+\alpha_2)^2-\lambda\,\mathrm{Pr}(\pi+\alpha_2)+S\lambda\,\mathrm{Pr}-\pi^2,\ l_6=(-\pi+\alpha_2)^2-\lambda\,\mathrm{Pr}(-\pi+\alpha_2)+S\lambda\,\mathrm{Pr}-\pi^2,$$

$$l_7=(r_1+\alpha_2)^2-\lambda\,\mathrm{Pr}(r_1+\alpha_2)+S\lambda\,\mathrm{Pr}-\pi^2,\ l_8=(r_2+\alpha_2)^2-\lambda\,\mathrm{Pr}(r_2+\alpha_2)+S\lambda\,\mathrm{Pr}-\pi^2,$$

$$l_9=\phi_2(\pi+\alpha_3)^2-\lambda\,\mathrm{Pr}(\pi+\alpha_3)+S\lambda\,\mathrm{Pr}-\phi_2\pi^2,$$

$$l_{10}=\phi_2(-\pi+\alpha_3)^2-\lambda\,\mathrm{Pr}(-\pi+\alpha_3)+S\lambda\,\mathrm{Pr}-\phi_2\pi^2,$$

$$l_{11}=\phi_2(s+\alpha_3)^2-\lambda\,\mathrm{Pr}(s+\alpha_3)+S\lambda\,\mathrm{Pr}-\phi_2\pi^2,$$

$$l_{12}=\phi_2(-s+\alpha_3)^2-\lambda\,\mathrm{Pr}(-s+\alpha_3)+S\lambda\,\mathrm{Pr}-\phi_2\pi^2,$$

$$l_{13}=\phi_2(\pi+\alpha_4)^2-\lambda\,\mathrm{Pr}(\pi+\alpha_4)+S\lambda\,\mathrm{Pr}-\phi_2\pi^2,$$

$$l_{14}=\phi_2(-\pi+\alpha_4)^2-\lambda\,\mathrm{Pr}(-\pi+\alpha_4)+S\lambda\,\mathrm{Pr}-\phi_2\pi^2,$$

$$l_{15}=\phi_2(s+\alpha_4)^2-\lambda\,\mathrm{Pr}(s+\alpha_4)+S\lambda\,\mathrm{Pr}-\phi_2\pi^2,$$

$$l_{16}=\phi_2(-s+\alpha_4)^2-\lambda\,\mathrm{Pr}(-s+\alpha_4)+S\lambda\,\mathrm{Pr}-\phi_2\pi^2,$$

$$m_1=-\lambda\,\mathrm{Pr}\left[\begin{array}{l}a_1\alpha_1\left(\dfrac{A_1e^{(\pi+\alpha_1)}}{l_1}+\dfrac{A_2e^{(-\pi+\alpha_1)}}{l_2}+\dfrac{A_3e^{(r_1+\alpha_1)}}{l_3}+\dfrac{A_4e^{(r_2+\alpha_1)}}{l_4}\right)\\ +a_2\alpha_2\left(\dfrac{A_1e^{(\pi+\alpha_2)}}{l_5}+\dfrac{A_2e^{(-\pi+\alpha_2)}}{l_6}+\dfrac{A_3e^{(r_1+\alpha_2)}}{l_7}+\dfrac{A_4e^{(r_2+\alpha_2)}}{l_8}\right)\end{array}\right],$$

$$m_2=-\lambda\,\mathrm{Pr}\left[\begin{array}{l}a_3\alpha_3\left(\dfrac{B_1e^{-a(\pi+\alpha_3)}}{l_9}+\dfrac{B_2e^{-a(-\pi+\alpha_3)}}{l_{10}}+\dfrac{B_3e^{-a(s+\alpha_3)}}{l_{11}}+\dfrac{B_4e^{-a(-s+\alpha_3)}}{l_{12}}\right)\\ +a_4\alpha_4\left(\dfrac{B_1e^{-a(\pi+\alpha_4)}}{l_{13}}+\dfrac{B_2e^{-a(-\pi+\alpha_4)}}{l_{14}}+\dfrac{B_3e^{-a(s+\alpha_4)}}{l_{15}}+\dfrac{B_4e^{-a(-s+\alpha_4)}}{l_{16}}\right)\end{array}\right]$$

$$m_3=\lambda\,\mathrm{Pr}\left[a_1\alpha_1\left(\frac{A_1}{l_1}+\frac{A_2}{l_2}+\frac{A_3}{l_3}+\frac{A_4}{l_4}\right)+a_2\alpha_2\left(\frac{A_1}{l_5}+\frac{A_2}{l_6}+\frac{A_3}{l_7}+\frac{A_4}{l_8}\right)\right],$$

$$m_4=\lambda\,\mathrm{Pr}\left[a_3\alpha_3\left(\frac{B_1}{l_9}+\frac{B_2}{l_{10}}+\frac{B_3}{l_{11}}+\frac{B_4}{l_{12}}\right)+a_4\alpha_4\left(\frac{B_1}{l_{13}}+\frac{B_2}{l_{14}}+\frac{B_3}{l_{15}}+\frac{B_4}{l_{16}}\right)\right],$$

$$m_5=\lambda\,\mathrm{Pr}\left[\begin{array}{l}a_1\alpha_1\left(\dfrac{A_1(\pi+\alpha_1)}{l_1}+\dfrac{A_2(-\pi+\alpha_1)}{l_2}+\dfrac{A_3(r_1+\alpha_1)}{l_3}+\dfrac{A_4(r_2+\alpha_1)}{l_4}\right)\\ +a_2\alpha_2\left(\dfrac{A_1(\pi+\alpha_2)}{l_5}+\dfrac{A_2(-\pi+\alpha_2)}{l_6}+\dfrac{A_3(r_1+\alpha_2)}{l_7}+\dfrac{A_4(r_2+\alpha_2)}{l_8}\right)\end{array}\right],$$

$$m_6 = \lambda \Pr \left[\begin{array}{l} a_3\alpha_3\left(\dfrac{B_1(\pi+\alpha_3)}{l_9} + \dfrac{B_2(-\pi+\alpha_3)}{l_{10}} + \dfrac{B_3(s+\alpha_3)}{l_{11}} + \dfrac{B_4(-s+\alpha_3)}{l_{12}} \right) \\ +a_4\alpha_4\left(\dfrac{B_1(\pi+\alpha_4)}{l_{13}} + \dfrac{B_2(-\pi+\alpha_4)}{l_{14}} + \dfrac{B_3(s+\alpha_4)}{l_{15}} + \dfrac{B_4(-s+\alpha_4)}{l_{16}} \right) \end{array} \right],$$

$$m_7 = m_1 e^{-\alpha_6} - m_2 e^{a\alpha_8} + m_3 - m_4,\ m_8 = m_1\alpha_6 e^{-\alpha_6} - m_2\alpha_8 e^{a\alpha_8} + m_5 - m_6,$$

$$\beta = \left(1 - e^{a(\alpha_8-\alpha_7)}\right)\left(\alpha_5 - \alpha_6 e^{(\alpha_5-\alpha_6)}\right) - \left(\alpha_7 - \alpha_8 e^{a(\alpha_8-\alpha_7)}\right)\left(1 - e^{(\alpha_5-\alpha_6)}\right),$$

$$a_5 = \frac{m_7\left(\alpha_7 - \alpha_8 e^{a(\alpha_8-\alpha_7)}\right) - m_8\left(1 - e^{a(\alpha_8-\alpha_7)}\right)}{\beta},\ a_6 = e^{-\alpha_6}\left(m_1 - a_5 e^{\alpha_5}\right),\ a_7 = \frac{a_5\left(1 - e^{(\alpha_5-\alpha_6)}\right) + m_7}{1 - e^{a(\alpha_8-\alpha_7)}},$$

$$a_8 = e^{a\alpha_6}\left(m_2 - a_7 e^{-a\alpha_7}\right).$$

Authors' affiliations:

D. S. Chauhan (**corresponding author**)

Department of Mathematics, University of Rajasthan, Jaipur – 302004, India

E-mail: dileepschauhan@gmail.com

V. Kumar

Department of Mathematics, University of Rajasthan, Jaipur – 302004, India

E-mail: vkagarwaluor@gmail.com